

Long Noncoding RNA SChLAP1 Accelerates the Proliferation and Metastasis of Prostate Cancer via Targeting miR-198 and Promoting the MAPK1 Pathway

Ye Li,*†‡§ Haihong Luo,§ Nan Xiao,* Jianmin Duan,* Zhiping Wang,* and Shuanke Wang¶¶

*Department of Urology, Lanzhou University Second Hospital, Lanzhou, P.R. China

†Key Laboratory of Urological Diseases, Lanzhou University, Lanzhou, P.R. China

‡Gansu Nephro-Urological Clinical Center, Lanzhou, P.R. China

§Department of Medical Services, Lanzhou University Second Hospital, Lanzhou, P.R. China

¶¶Department of Orthopedics, Lanzhou University Second Hospital, Lanzhou, P.R. China

Prostate cancer has become the most commonly diagnosed and the second leading cause of cancer-related deaths in males. The long noncoding RNA second chromosome locus associated with prostate-1 (SChLAP1) has been found to be overexpressed in a subset of prostate cancer. However, the significance and mechanism of SChLAP1 in prostate cancer are not well known. In this study, we explored the role of SChLAP1 in prostate cancer tissues, cell lines, and mouse models. The effect of SChLAP1 on miR-198 and MAPK1 was specifically examined. We found that SChLAP1 expression was significantly increased in prostate cancer cells and tissues. Knockdown of SChLAP1 promoted apoptosis and inhibited cell proliferation and invasion in vitro and in vivo. In addition, a potential bonding site between miR-198 and SChLAP1 was predicted, and a low expression of miR-198 was found in prostate cancer tissues and cells. Knockdown of SChLAP1 significantly increased the expression of miR-198, and SChLAP1 overexpression markedly decreased it, indicating that SChLAP1 acted as a negative regulator in the expression of miR-198. Furthermore, our results showed that SChLAP1 interacted with miR-198 and subsequently modulated the MAPK1 signaling pathway in prostate cancer. In conclusion, our study has identified a novel pathway through which SChLAP1 exerts its oncogenic role in prostate cancer at the level of miRNAs and provided a molecular basis for potential applications of SChLAP1 in the prognosis and treatment of prostate cancer.

Key words: Second chromosome locus associated with prostate-1 (SChLAP1); miR-198; MAPK1; Prostate cancer

INTRODUCTION

Prostate cancer is the most common malignancy in males and accounts for 13% of cancer-related deaths¹. A majority of prostate tumors are slow growing, nonlethal, and usually cured by definitive treatment. However, there are a small number of patients who experience disease recurrence after first-line treatments, which may lead to metastasis and death²⁻⁴. Therefore, early screening for prostate cancer is significant for its prevention and treatment.

Long noncoding RNAs (lncRNAs) are a type of RNA transcript that are longer than 200 nucleotides in length and are implicated in multiple biological processes⁵. Recently, lncRNAs were recognized to be diagnostic and prognostic biomarkers for malignant tumors^{6,7}. Second chromosome locus associated with prostate-1 (SChLAP1) is one of the most important lncRNAs. It was first identified by Prensner et al. and is located in the nucleus⁸.

Previous studies have demonstrated that SChLAP1 is highly overexpressed in a subset of prostate cancers and is associated with lethal disease⁹. However, little is known about the exact mechanism of SChLAP1 in prostate cancer development.

MicroRNAs (miRNAs) are a conserved family of small noncoding RNA molecules that posttranscriptionally regulate gene expression¹⁰. It was estimated that about 60% of genes can be regulated by miRNAs¹¹. miR-198 is a recently identified cancer-related miRNA. It was reported to be downregulated in many cancers, such as hepatocellular carcinoma¹², lung cancer¹³, pancreatic cancer¹⁴, and ovarian cancer¹⁵. Its overexpression has been detected in retinoblastoma¹⁶ and esophageal cancer¹⁷. In addition, miR-198 may suppress the proliferation and invasion of colorectal carcinoma¹⁸. A recent study identified that miR-198 negatively regulated Livin expression in prostate

cancer cell lines¹⁹. However, the exact expression of miR-198 and the molecular mechanism underlying its role in prostate cancer require further exploration.

Many studies have demonstrated that the mitogen-activated protein kinases (MAPKs) play an important role in regulating cancer cell invasion and metastasis²⁰. MAPKs have been implicated in a wide array of physiological processes including cell growth, differentiation, and apoptosis²¹. In addition, it was reported that ARF1 promoted prostate tumorigenesis via targeting MAPK signaling²². More importantly, forced expression of miR-198 significantly decreased p44/42 MAPK activation in both HepG2 and Hep3B cells¹², implying that miR-198 might exert its anticancer effect through the inhibition of the MAPK signaling pathway.

In this study, we explored the impact of SchLAP1 in prostate cancer tissues, cell lines, and mouse models. The effect of SchLAP1 on miR-198 and MAPK1 was specifically examined.

MATERIALS AND METHODS

Tissue Samples

Prostate tissues were obtained from the Radical Prostatectomy Series and Rapid Autopsy Program at the Tissue Core of the Lanzhou University Second Hospital. All tissue samples were collected with informed consent under an institutional review board (IRB)-approved protocol at the Lanzhou University Second Hospital.

Cell Culture

RWPE-1, LNCap, 22Rv1, DU145, and PC-3 cells (ATCC, Rockville, MD, USA) were grown in DMEM complemented with 10% FBS (v/v; Life Technologies, Grand Island, NY, USA). All cells were cultured at 37°C in a 5% CO₂ incubator.

Quantitative Real-Time Polymerase Chain Reaction (qRT-PCR)

Total RNA was extracted from cells or tissues using TRIzol reagent (Invitrogen, Carlsbad, CA, USA) according to the manufacturer's instructions. Equal amounts of RNA were reversely transcribed to cDNA with the SuperScript Reverse Transcriptase Kit (Thermo Fisher Scientific, Waltham, MA, USA). Total cDNA was then amplified and analyzed by SYBR Green PCR Master Mix (Thermo Fisher Scientific) in a Fast Real-time PCR 7500 System (Applied Biosystems, Foster City, CA, USA). The following primers were used: SchLAP1, 5'-TGGACACAATTTCAAGTCCTCA-3' (forward) and 5'-CATGGTGAAAGTGCCTTATACA-3' (reverse); miR-198, 5'-GAATTCCAGTACTCGGTAGTTGTCTGG-3' (forward) and 5'-GGTACCGCGGTGCTTTTCCAATC TGC-3' (reverse). The original Ct (cycle of the threshold)

values were adjusted to GAPDH. Data were converted and presented as fold changes related to the control.

Northern Blot

Total RNA was denatured with 1 M glyoxal and 50% DMSO, electrophoresed on agarose gel, and transferred onto Hybond N⁺ membrane (GE Healthcare, Piscataway, NJ, USA). After baking at 80°C for 2 h, the blot was hybridized overnight with ³²P-labeled probe (2 ng/ml) and 200 mg/ml salmon sperm DNA at 60°C. The membrane was then washed twice, and the positive bands were detected after autoradiography using Quantity One (Bio-Rad, Hercules, CA, USA). Fluorescence intensity was measured by the ImageJ software.

Cell Viability Analysis

PC-3 cells were cultured on a 96-well plate and transfected with SchLAP1-siRNA for various times. Cell viability was then measured by the CCK-8 Kit (Beyotime Biotechnology, Shanghai, P.R. China) according to the manufacturer's instructions.

Flow Cytometry Analysis of Apoptosis

PC-3 cells were transfected with SchLAP1-siRNA for 24 h. After washing with ice-cold PBS, the cells were resuspended in annexin V binding buffer and incubated with FITC-conjugated annexin V antibody (Cell Signaling Technology, Danvers, MA, USA) and propidium iodide (1:100 dilutions) for 15 min at room temperature. The cells were then analyzed with a Beckman Counter.

Western Blot

Total protein samples from cells and tissues were prepared using the standard protocol. Equivalent amounts of protein samples were separated by 10% SDS-PAGE and transferred to PVDF membranes (Millipore, Billerica, MA, USA). Membranes were then incubated at room temperature with 5% nonfat dry milk dissolved in T-BST. The blots were probed overnight with respective primary antibodies (Abcam, Cambridge, UK) at 4°C and then incubated with HRP-conjugated secondary antibodies (Beyotime Biotechnology) at room temperature. Membranes were extensively washed several times. Proteins were detected using a ChemiDoc XRS imaging system and Quantity One analysis software (Bio-Rad). GAPDH was used as an endogenous reference.

Cell Migration and Invasion Analyses

PC-3 cells transfected with SchLAP1-siRNA or scramble were cultured in a 24-well chamber. The confluent cell monolayer was stroked with a pipette tip. Cells were washed to remove detached and damaged cells and then cultured for 24 h. Cell migration was monitored microscopically, and the migration distance was

measured from five preset positions for each treatment condition using the ImageJ software.

The invasion capacity of PC-3 cells was examined using a Transwell invasion assay. Briefly, cells were plated in the upper chamber in serum-free medium, and 20% FBS was added to the medium in the lower chamber. After incubating for 24 h, noninvading cells were removed from the top well with a cotton swab, while the bottom cells were fixed in 95% ethanol and stained with hematoxylin. The cell numbers were determined by counting of the penetrating cells under a microscope at 200× magnification on 10 random fields in each well.

Bioinformatics Data Set

Prediction of the interaction between miR-198 and SchLAP1 or MAPK1 was performed using DIANA TOOLS (<http://diana.imis.athena-innovation.gr/DianaTools>) as previously described²³.

Luciferase Reporter Assay

The 3'-UTR of SchLAP1 mRNA containing miR-198 binding sites was PCR amplified and inserted downstream of a *Renilla* luciferase reporter gene in the pGL3 vector. A mutant construct containing mutations within the binding sites was generated using the TaKaRa MutanBEST Kit (TaKaRa, Shiga, Japan) according to the manufacturer's instructions. PC-3 cells were cotransfected with miR-198 mimics and wild-type or mutant luciferase reporter plasmid by Lipofectamine 2000 reagent (Invitrogen). Twenty-four hours after transfection, the luciferase activities were measured with a dual-luciferase reporter assay system (Promega, Madison, WI, USA) according to the manufacturer's instructions. *Renilla* luciferase intensity was normalized to firefly luciferase intensity.

Animal Work and Experimental Protocols

Male athymic BALB/c mice (Laboratory Animal Center of Lanzhou University, Lanzhou, P.R. China) were used in the present studies. Mice were housed under controlled conditions (25±2°C, 70% humidity, and 12-h light–dark periods) and fed with a regular sterile chow diet and water ad libitum. The experimental protocol was in accordance with the guidelines of the Institutional Animal Care and Use Committee (IACUC) of Lanzhou University. All mice were randomly divided into two groups. One group was subcutaneously inoculated in the back with 5×10⁶ PC-3 cells that had been transfected with SchLAP1-siRNA, and the other group was treated with scrambled PC-3 cells. Animals were monitored for signs of tumor growth. Tumor volumes were calculated at 5–30 days after injection according to the formula: [length (mm)×width (mm)×width (mm)×0.52]²⁴. Upon termination, tumors were harvested, and tumor proteins were analyzed by Western blot.

Immunohistochemistry

Tumor sections were prepared essentially as previously described²⁵. The sections were incubated with VEGF antibody (Cell Signaling Technology) overnight at 4°C, followed by incubation with fluorophore-conjugated secondary antibody (Invitrogen) for 1 h. Sections were visualized with a fluorescence microscope.

Statistical Analysis

All results were presented as mean±SD. The statistical significance of the studies was analyzed using Student's *t*-test. The difference was considered to be statistically significant with a value of *p*<0.05.

RESULTS

SchLAP1 Is Highly Expressed in Prostate Cancer Cells

To understand the biological significance of lncRNA SchLAP1 in prostate cancer, the mRNA levels of SchLAP1 were examined in prostate cancer tissues and their corresponding noncancerous tissues from 40 patients. The results showed that the expression of SchLAP1 was significantly higher in prostate cancer tissues than in normal tissues (*p*<0.01) (Fig. 1A). The expression of SchLAP1 was subsequently measured in RWPE-1 cells and four prostate cancer cell lines (LNCap, 22Rv1, DU145, and PC-3). The mRNA expression level of SchLAP1 was significantly increased in prostate cancer cells compared with RWPE-1 cells (*p*<0.01) (Fig. 1B). Furthermore, Northern blot analysis was performed to determine the transcription level of SchLAP1. Likewise, the transcription of SchLAP1 was remarkably increased in prostate cancer tissues (*p*<0.01) (Fig. 1C and E) and cell lines (*p*<0.01) (Fig. 1D and F). These results indicated that SchLAP1 was highly expressed in prostate cancer cells.

SchLAP1 Knockdown Increases Apoptosis in Prostate Cancer Cells

Based on the above observations, we next investigated the role of SchLAP1 in prostate cancer cell proliferation. An siRNA specific for SchLAP1 was designed and transfected into LNCap and PC-3 cells. According to qRT-PCR and Northern blot analysis, the relative mRNA level of SchLAP1 was significantly decreased after the transfection of SchLAP1-siRNA (*p*<0.01) (Fig. 2A). This revealed that the SchLAP1-siRNA used in the present study successfully knocked down SchLAP1 in LNCap and PC-3 cells. To determine the role of SchLAP1 in prostate cancer cell growth, cells transfected with SchLAP1-siRNAs were used in the CCK-8 assay. siRNA-mediated knockdown of SchLAP1 significantly decreased cell proliferation after 48 or 72 h posttransfection in LNCap and PC-3 cells, respectively

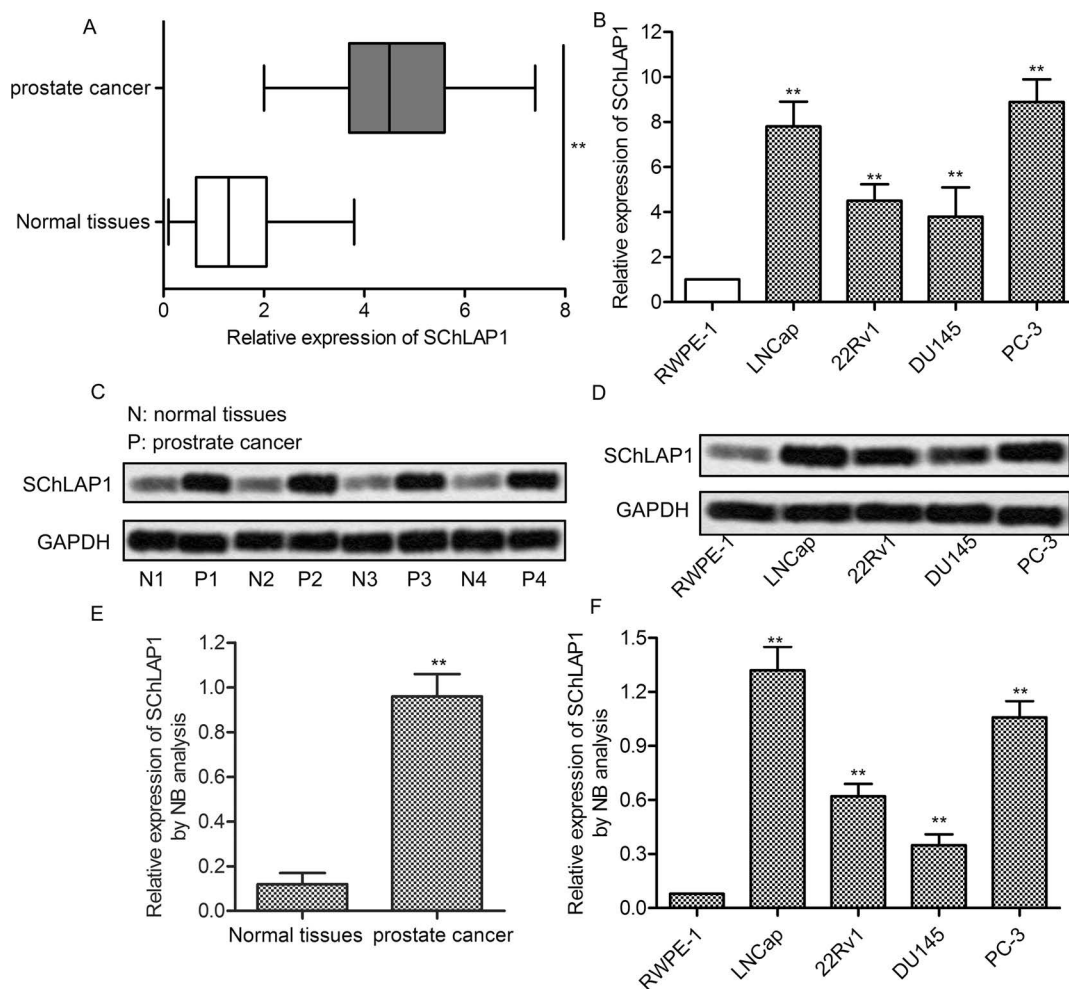


Figure 1. Second chromosome locus associated with prostate-1 (SCHLAP1) is highly expressed in prostate cancer cells. (A) The mRNA levels of SCHLAP1 in 40 prostate cancer tissues and adjacent normal tissues were assayed by quantitative real-time polymerase chain reaction (qRT-PCR). (B) The mRNA levels of SCHLAP1 in RWPE-1, LNCap, 22Rv1, DU145, and PC-3 cells were assayed by qRT-PCR. (C) Northern blot analysis of SCHLAP1 in normal and prostate cancer tissues. The samples from four randomly selected patient tumors are presented. (D) The mRNA levels of SCHLAP1 in RWPE-1, LNCap, 22Rv1, DU145, and PC-3 cells were assayed by Northern blot. (E) Quantification of (C). (F) Quantification of (D). All the experiments were repeated at least three times. GAPDH was used as a loading control. ** $p < 0.01$ versus normal cells or tissues.

($p < 0.05$) (Fig. 2B and C). In addition, the expression level of proliferation-associated proteins was measured in SCHLAP1-siRNA-treated cells. The expression level of Ki-67 and PCNA was obviously decreased in SCHLAP1-siRNA-treated LNCap and PC-3 cells ($p < 0.01$) (Fig. 2D–F). On the other hand, flow cytometry analysis showed that SCHLAP1 knockdown significantly increased the percentage of annexin V⁺ apoptotic cells ($p < 0.01$) (Fig. 2G and H). Undoubtedly, the apoptosis-associated proteins caspase 3 and caspase 9 were markedly increased in SCHLAP1-siRNA-treated LNCap and PC-3 cells ($p < 0.01$) (Fig. 2I–K). Taken together, these results indicate that SCHLAP1 knockdown may inhibit proliferation and promote apoptosis in prostate cancer cells.

SCHLAP1 Knockdown Suppresses the Migration and Invasion of Prostate Cancer Cells

To investigate the effect of SCHLAP1 on cell migration, a wound healing assay was carried out. The cell migration levels were significantly reduced in SCHLAP1 knockdown cells ($p < 0.01$) (Fig. 3A and B). Furthermore, the Matrigel Transwell assay was used to measure the invasion of prostate cancer cells. The capacity for cell invasion was obviously decreased in LNCap and PC-3 cells after SCHLAP1 suppression (Fig. 3C and D). Because VEGF and MMPs play an important role in tumor progression by promoting migration and invasion^{26,27}, the effect of SCHLAP1 knockdown on the expression levels of these proteins was determined in LNCap and PC-3 cells. As

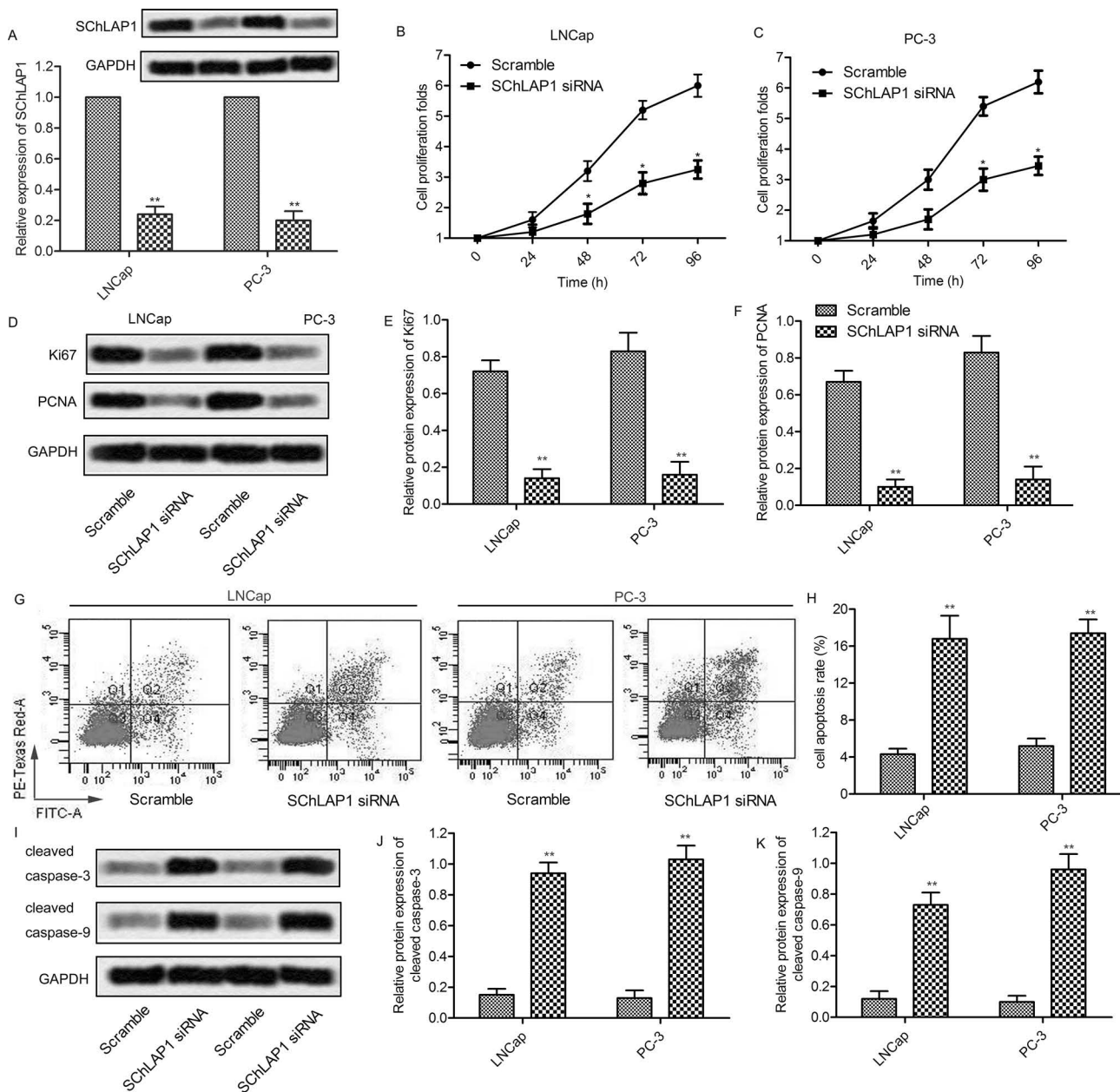


Figure 2. SCHLAP1 knockdown increases apoptosis in prostate cancer cells. (A) LNCap and PC-3 cells were transfected with SCHLAP1-siRNA or scramble for 24 h, and the mRNA levels of SCHLAP1 were measured by qRT-PCR and Northern blot. (B, C) LNCap and PC-3 cells were transfected with SCHLAP1-siRNA or scramble for 24, 48, 72, and 96 h, and cell viability was assayed by the CCK-8 kit. (D) Protein levels of Ki-67 and PCNA were assayed by Western blot. (E, F) Quantifications of (D). (G) The cell apoptosis was analyzed by annexin V flow cytometry. (H) Apoptotic cell quantification for three independent experiments. (I) Protein levels of caspase 3 and caspase 9 were assayed by Western blot. (J, K) Quantifications of (I). All the experiments were repeated at least three times, and representative data are shown. GAPDH was used as a loading control. * $p < 0.05$, ** $p < 0.01$ versus scramble.

anticipated, the expressions of MMP-9, MMP-14, and VEGF were significantly decreased after transfection with SCHLAP1-siRNA ($p < 0.001$) (Fig. 3E–H). Taken together, these findings indicate that SCHLAP1 knockdown may inhibit the migration and invasion of prostate cancer cells through the downregulation of migration-related proteins.

The Expression of miR-198 Is Decreased in Prostate Cancer Cells

Because miR-198 was a potential tumor suppressor in prostate cancer¹⁹, bioinformatics analysis was performed. There was an 18-bp matched sequence between miR-198 and SCHLAP1, indicating that they may have

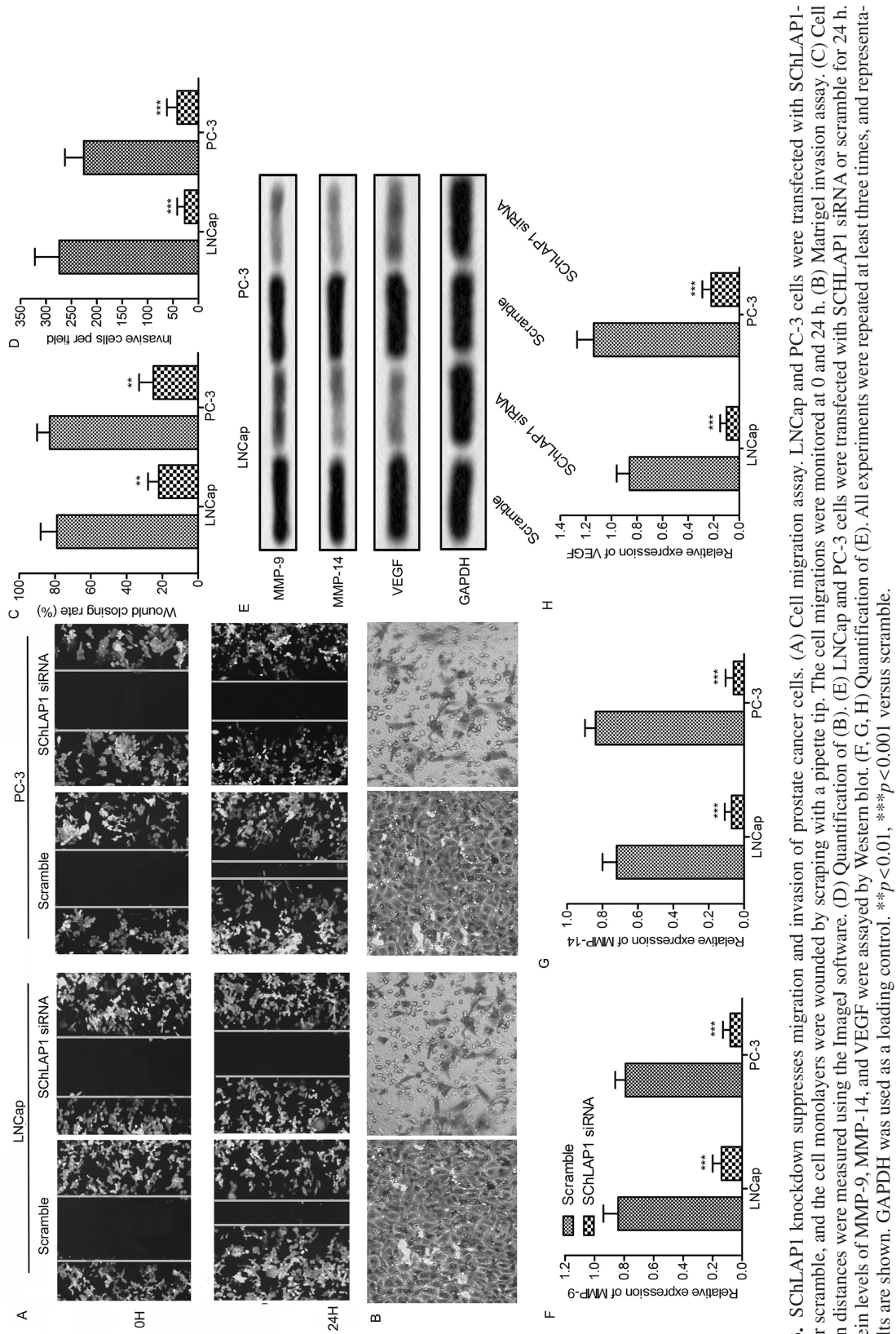


Figure 3. SCHLAP1 knockdown suppresses migration and invasion of prostate cancer cells. (A) Cell migration assay. LNCap and PC-3 cells were transfected with SCHLAP1-siRNA or scramble, and the cell monolayers were wounded by scraping with a pipette tip. The cell migrations were monitored at 0 and 24 h. (B) Matrigel invasion assay. (C) Cell migration distances were measured using the ImageJ software. (D) Quantification of (B). (E) LNCap and PC-3 cells were transfected with SCHLAP1 siRNA or scramble for 24 h. The protein levels of MMP-9, MMP-14, and VEGF were assayed by Western blot. (F, G, H) Quantification of (E). All experiments were repeated at least three times, and representative results are shown. GAPDH was used as a loading control. ** $p < 0.01$, *** $p < 0.001$ versus scramble.

target-specific selectivity (Fig. 4A). We then investigated the expression of miR-198 in prostate cancer tissues and their corresponding noncancerous tissues from 40 patients. The results showed that the expression of miR-198 in prostate cancer tissues was significantly lower than in normal tissues ($p < 0.01$) (Fig. 4B). As before, we subsequently compared the expression of miR-198 in RWPE-1 cells and prostate cancer cell lines (LNCap, 22Rv1, DU145, and PC-3). The mRNA expression level of miR-198 was significantly decreased in prostate cancer cells compared with RWPE-1 cells ($p < 0.01$) (Fig. 4C). Furthermore, according to Northern blot analysis, the transcription of miR-198 was remarkably increased in prostate cancer tissues (Fig. 4D) and cell lines (Fig. 4E) as well. Collectively, these results indicate that the expression of miR-198 was markedly decreased in prostate cancer cells.

The Interaction Between SChLAP1 and miR-198 Influences the Progression of Prostate Cancer

To further determine the relationship between SChLAP1 and miR-198, the expression level of miR-198 in cells

transfected with SChLAP1-siRNA was detected. The expression level of miR-198 was significantly increased in LNCap and PC-3 cells after SChLAP1 knockdown ($p < 0.001$) (Fig. 5A and B). Overexpression or inhibition of SChLAP1 and miR-198 was then carried out. The results showed that the inhibitor of miR-198 markedly inhibited its expression, but the inhibitory effect was reduced in the presence of SChLAP1-siRNA (Fig. 5C). Similarly, overexpression of SChLAP1 partially inhibited miR-198 mimic-induced miR-198 induction (Fig. 5D). To further determine the bonding effect between SChLAP1 and miR-198, a luciferase reporter containing exact or mutant miR23d binding sites was established. The results showed that the miR-198 mimic significantly decreased the luciferase activity of the wild-type SChLAP1 reporter plasmid ($p < 0.01$). However, the reducing effect of the miR-198 mimic was abolished on the mutant SChLAP1 reporter plasmid (Fig. 5E). In addition, SChLAP1 knockdown significantly reduced miR-198 inhibition-induced cell proliferation ($p < 0.01$) (Fig. 6F), migration ($p < 0.01$) (Fig. 6H), and invasion ($p < 0.01$) (Fig. 6I), and rebuilt the miR-198 inhibition-induced reduction of cell apoptosis

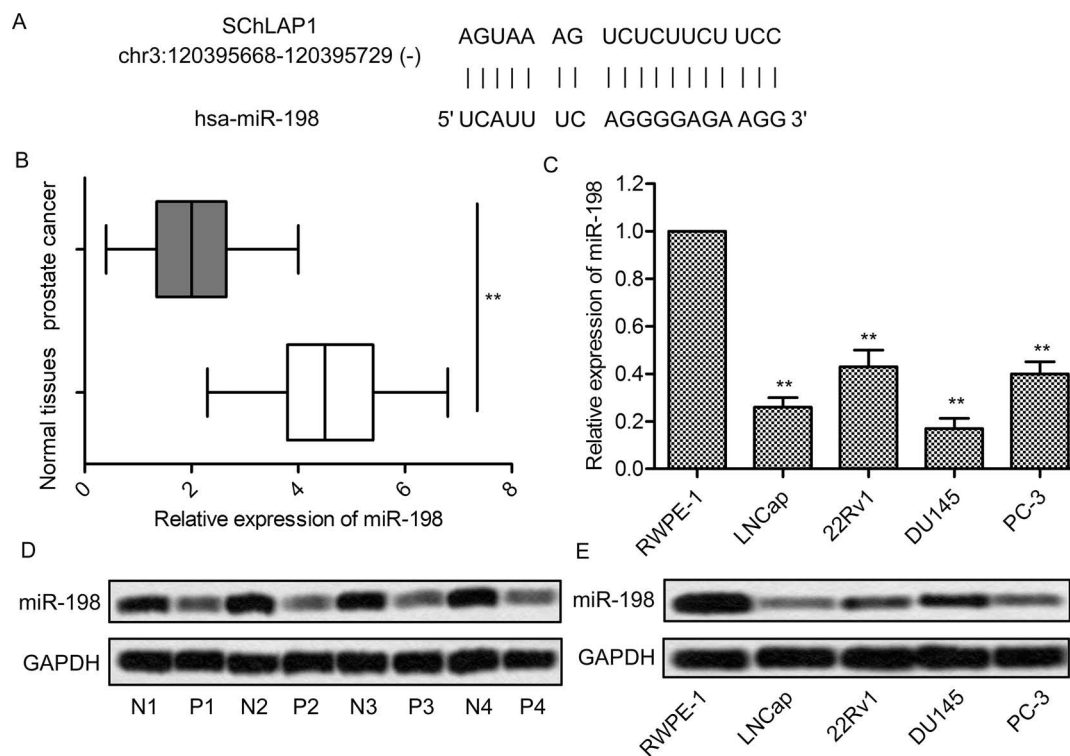


Figure 4. The expression of miR-198 is decreased in prostate cancer cells. (A) Bioinformatics analysis of SChLAP1 and miR-198. (B) The mRNA levels of miR-198 in 40 prostate cancer tissues and adjacent normal tissues were assayed by qRT-PCR. (C) The mRNA levels of miR-198 in RWPE-1, LNCap, 22Rv1, DU145, and PC-3 cells were assayed by qRT-PCR. (D) Northern blot analysis of miR-198 in normal and prostate cancer tissues. The samples from four randomly selected patient tumors are presented. (E) The mRNA levels of miR-198 in RWPE-1, LNCap, 22Rv1, DU145, and PC-3 cells were assayed by Northern blot. All experiments were repeated at least three times. GAPDH was used as a loading control. ** $p < 0.01$ versus normal cells or tissues.

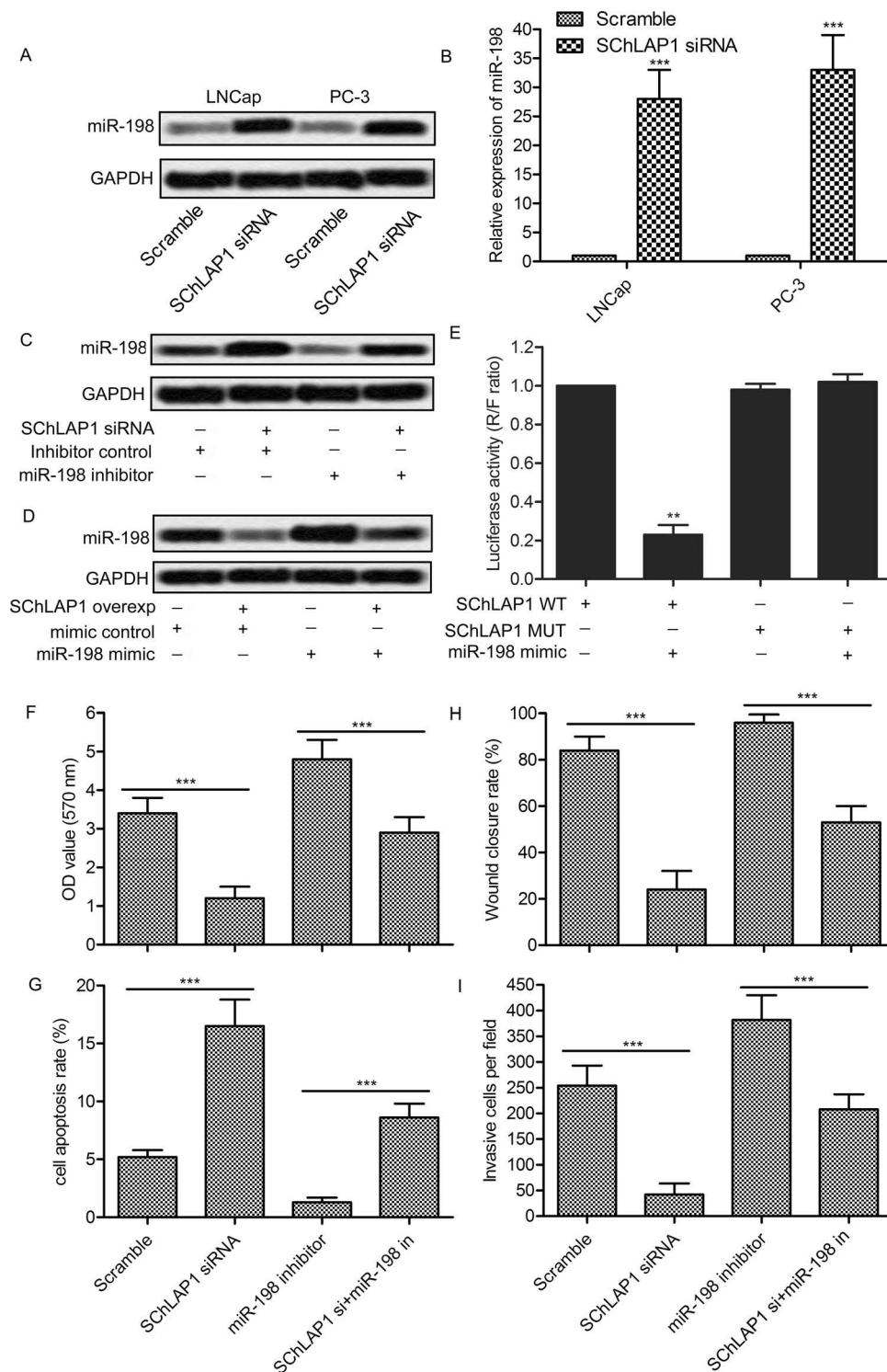


Figure 5. The interaction between SchLAP1 and miR-198 influences the progression of prostate cancer. (A, B) LNCap and PC-3 cells were transfected with SchLAP1-siRNA for 24 h, and the levels of miR-198 were measured by Northern blot (A) and qRT-PCR (B). (C) PC-3 cells were transfected with SchLAP1-siRNA and/or the miR-198 inhibitor for 24 h, and the levels of miR-198 were measured by Northern blot. (D) PC-3 cells were transfected with synthetic SchLAP1 and/or the miR-198 mimic for 24 h, and the levels of miR-198 were measured by Northern blot. (E) PC-3 cells were transfected with wild-type or mutant SchLAP1 reporter plasmid and cotransfected with the miR-198 mimic for 24 h. Cell lysates were assayed for luciferase activity. (F) Quantification of cell viability assay. (G) Quantification of cell apoptosis assay. (H) Quantification of cell migration. (I) Quantification of cell invasion. All experiments were repeated at least three times. GAPDH was used as a loading control. ** $p < 0.01$, *** $p < 0.001$.

($p < 0.01$) (Fig. 6). These results suggest that SChLAP1 may regulate the expression of miR-198 and subsequently influence the progression of prostate cancer.

SChLAP1 Activates the MAPK1 Signaling Pathway

Many studies have reported that MAPKs play an important regulatory role in cancer progression, and

our bioinformatics analysis indicated that miR-198 and MAPK1 had a targeted correlation (Fig. 6A). Based on this, we further investigated whether inhibition of SChLAP1 and/or miR-198 would affect the MAPK1 pathway. SChLAP1 knockdown significantly decreased the phosphorylation of MAPK1, whereas the inhibition of miR-198 had exactly the opposite effect ($p < 0.01$)

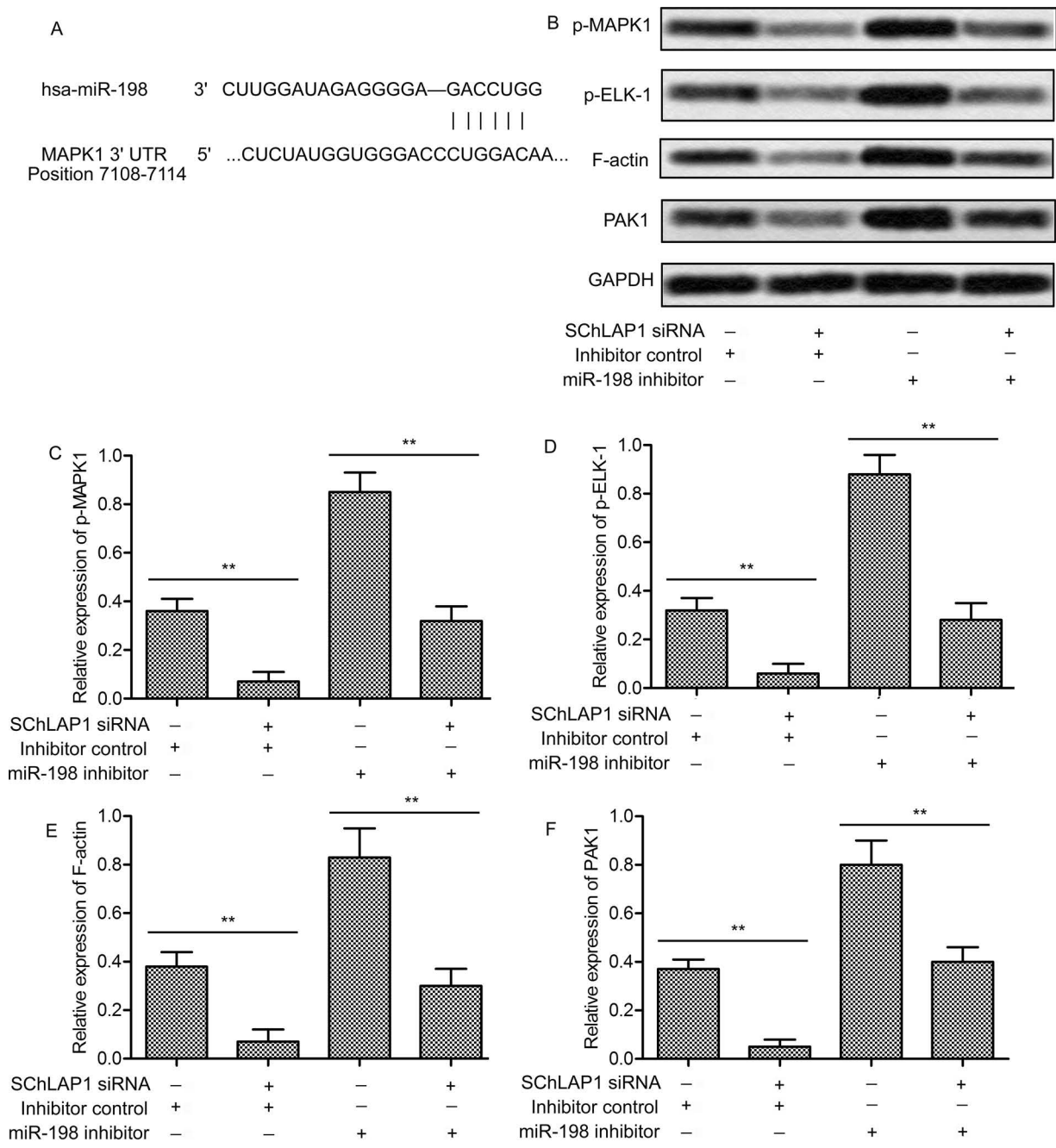


Figure 6. SChLAP1 activates the MAPK1 signaling pathway. (A) Bioinformatics analysis of miR-198 and MAPK1. (B) PC-3 cells were transfected with SChLAP1-siRNA and/or the miR-198 inhibitor for 24 h, and the levels of phosphorylated MAPK1, phosphorylated ELK-1, F-actin, and PAK1 were measured by Western blot. (C–F) Quantification of Figure 3B. All experiments were repeated at least three times. GAPDH was used as a loading control. $**p < 0.01$.

(Fig. 6B and C). In addition, SChLAP1-siRNA combined with the miR-198 inhibitor notably weakened the effect of the miR-198 inhibitor alone ($p < 0.01$). Since ELK-1, F-actin, and PAK1 are major target genes of MAPK1 and play an important role in cancer progression, the expression of phosphorylated ELK-1, F-actin, and PAK1 was examined. Unsurprisingly, the expression of these proteins showed changes similar to p-MAPK1

($p < 0.01$) (Fig. 6B and D–F). These results indicate that the interaction of SChLAP1 and miR-198 may contribute to MAPK1 activation.

SChLAP1 Knockdown Relieves Tumor Growth and Metastasis In Vivo

We next assessed the role of SChLAP1 on tumor progression in a mouse model for prostate cancer. The

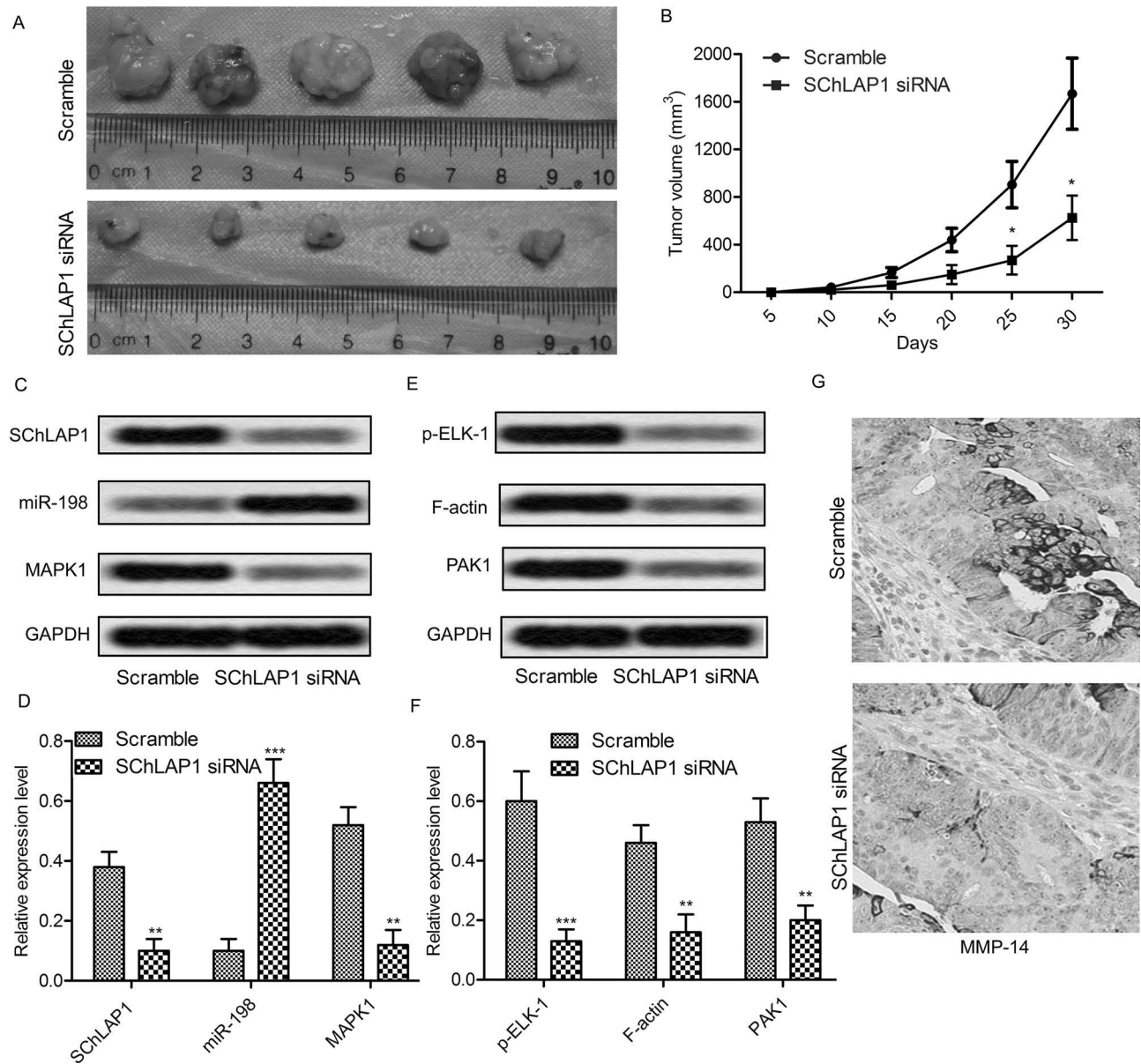


Figure 7. SChLAP1 knockdown relieves tumor growth and metastasis in vivo. (A) Male mice were injected intraperitoneally with SChLAP1 knockdown or scramble PC-3 cells; the tumor size was measured using a ruler at 30 days. (B) Calculation of tumor volume at 5, 10, 15, 20, 25, and 30 days after injection. (C) Northern blot analysis of SChLAP1, miR-198, and MAPK1 in the tumor tissues. (D) Quantitation of (C). (E) Western blot analysis of phosphorylated ELK-1, F-actin, and PAK1 in the tumor tissues. (F) Quantitation of (E). (G) immunohistochemistry analysis of MMP-14 in the tumor tissues. All experiments were repeated at least three times. GAPDH was used as a loading control. * $p < 0.05$, ** $p < 0.01$, *** $p < 0.001$ versus control tissues.

tumor volume in the SChLAP1 knockdown mouse model was markedly smaller than in the scrambled model at 25–30 days ($p < 0.01$) (Fig. 7A and B). The Northern blot results showed that tissues from the SChLAP1 knockdown mouse model exhibited a higher miR-198 expression and a lower MAPK1 expression when compared to the scrambled model ($p < 0.001$) (Fig. 7C and D). In addition, the Western blot showed that expression of p-ELK-1, F-actin, and PAK1 was decreased in the SChLAP1 knockdown mouse model ($p < 0.01$) (Fig. 7E and F). Furthermore, immunohistochemistry staining showed that the expression of migration-related protein MMP-14 was significantly decreased in the SChLAP1 knockdown mouse model (Fig. 7G). Taken together, these results indicate that SChLAP1 modulates tumor growth and migration via the miR-198/MAPK1 signaling pathway.

DISCUSSION

In this study, we investigated the role of SChLAP1 in prostate cancer and have made several novel observations. (1) SChLAP1 is highly expressed in prostate cancer and closely related to tumor progression. (2) miR-198 has a low expression in prostate cancer cells. (3) SChLAP1 can target and downregulate the expression of miR-198. (4) miR-198 and MAPK1 are involved in the tumor-promoting effect of SChLAP1.

Accumulating evidence suggests that lncRNAs play diverse roles in human carcinoma^{28,29}. Recently, many lncRNAs have been linked to tumorigenesis, either as oncogenes or tumor suppressors. Although the underlying mechanism of many of these lncRNAs remains to be elucidated, it is clear that lncRNAs contribute to the dysregulation of gene expression in prostate cancer, which then results in cancer initiation, development, and progression³⁰.

One of the first lncRNAs discovered to be highly upregulated in prostate cancer was prostate cancer antigen 3 (PCA3), which was initially discovered via expression profiling of a prostate sample³¹. Recently, SChLAP1 was found to be overexpressed in a subset of prostate cancers. SChLAP1 levels independently predict poor outcomes, including metastasis and prostate cancer-specific mortality⁸. SChLAP1 was also overexpressed in bladder cancer and resulted in cell growth arrest, apoptosis induction, and migration inhibition³². In the present work, we found that there was also a significant increase in SChLAP1 expression in prostate cancer samples compared with their adjacent histologically normal tissues, and similar results were observed in the corresponding cell lines and mouse models. Furthermore, our studies found that SChLAP1 knockdown significantly accelerated apoptosis and suppressed the migration and invasion abilities of prostate cancer cells. The expression of cell migration-related proteins MMP-9/MMP-14/VEGF was obviously

inhibited by SChLAP1 knockdown. This provided strong evidence that SChLAP1 acts as an oncogene in human prostate cancer.

Previous research has demonstrated the tumor-suppressive functions of miR-198 in various human cancers such as esophageal, gastric, and pancreatic cancers^{14,17,33}. In addition, the mechanism of the tumor-suppressive functions of miR-198 has also been investigated by many researchers. Wang et al. demonstrated that miR-198 repressed tumor growth and metastasis in colorectal cancer by targeting fucosyl transferase¹⁸. Yang et al. found that miR-198 inhibited proliferation and induced apoptosis of lung cancer cells via targeting FGFR1¹³. However, very few studies have addressed the function of miR-198 in prostate cancer. There has only been a study showing that Livin expression may be downregulated by miR-198 in human prostate cancer cell lines. In our study, we first found that the expression of miR198 was markedly decreased in prostate cancer tissues and cell lines compared with normal paired samples. Furthermore, the potential target domain between miR-198 and SChLAP1 was predicted by bioinformatics analysis, and the negative correlation between them was confirmed in vitro and in vivo. These findings not only testified to the regulatory role but also presented a potential upstream target for miR-198 in prostate cancer.

Numerous studies have demonstrated that MAPK signaling pathways play an important role in prostate cancer growth and metastasis^{34,35}. There are three conserved MAPKs, including c-jun NH₂-terminal kinases (JNK), extracellular signal-regulated kinases (ERKs), and the p38 groups³⁶. In particular, MAPK/ERK activation is strongly linked to cell growth, proliferation, survival, and differentiation³⁷. Several studies have indicated that suppression of MAPKs had the potential to prevent invasion and metastasis in various cancers^{20,38}. In addition, some miRNAs are involved in the regulation of MAPKs, such as miR-198¹². In our study, we first found a potential binding domain between miR-198 and MAPK1. SChLAP1 knockdown, which caused miR-198 upregulation, significantly inhibited the phosphorylation of MAPK1. On the contrary, the inhibition of miR-198 notably increased the phosphorylation of MAPK1. Accordingly, the downstream genes of MAPKs went along with the change of MAPK1. Furthermore, an in vivo study also showed that SChLAP1 knockdown could increase miR-198 expression, inhibit MAPK1 signaling, and subsequently inhibit tumor cell growth and metastasis.

In vitro and in vivo gain-of-function and loss-of-function experiments indicate that SChLAP1 is critical for cancer cell invasiveness and metastasis by antagonizing the genome-wide localization and regulatory functions of the SWI/SNF chromatin-modifying complex⁸. In this study, we have proposed a new mechanism through which

SChLAP1 exerts its oncogenic role in prostate cancer at the level of miRNAs. Our results revealed that SChLAP1 may competitively bind miR-198 and modulate the expression of MAPK1 indirectly in prostate cancer cells. Understanding the precise molecular mechanism is vital for exploring new potential strategies for early diagnosis and therapy. Our experimental data also suggest that targeting the SChLAP1–miR198–MAPK1 axis may represent a novel therapeutic application in prostate cancer.

ACKNOWLEDGMENT: This work was supported by a research grant from the National Natural Science Foundations of China (81400760). The authors declare no conflicts of interest.

REFERENCES

1. Siegel RL, Miller KD, Jemal A. Cancer statistics, 2016. *Ca A Cancer J Clin.* 2016;66(1):7.
2. Etzioni R, Cha R, Feuer EJ, Davidov O. Asymptomatic incidence and duration of prostate cancer. *Am J Epidemiol.* 1998;148(8):775–85.
3. Makarov DV, Humphreys EB, Mangold LA, Carducci MA, Partin AW, Eisenberger MA, Walsh PC, Trock BJ. The natural history of men treated with deferred androgen deprivation therapy in whom metastatic prostate cancer developed following radical prostatectomy. *J Urol.* 2008;179(1):156–61; discussion 161–2.
4. Pound CR, Partin AW, Eisenberger MA, Chan DW, Pearson JD, Walsh PC. Natural history of progression after PSA elevation following radical prostatectomy. *JAMA* 1999;281(17):1591–7.
5. Zhao XY, Lin JD. Long noncoding RNAs: A new regulatory code in metabolic control. *Trends Biochem Sci.* 2015;40(10):586–96.
6. Schwarzenbach H, Hoon DSB, Pantel K. Cell-free nucleic acids as biomarkers in cancer patients. *Nat Rev Cancer* 2011;11(6):426–37.
7. Crowley E, Di NF, Loupakis F, Bardelli A. Liquid biopsy: Monitoring cancer-genetics in the blood. *Nat Rev Clin Oncol.* 2013;10(8):472–84.
8. Prensner JR, Iyer MK, Sahu A, Asangani IA, Cao Q, Patel L, Vergara IA, Davicioni E, Erho N, Ghadessi M. The long noncoding RNA SChLAP1 promotes aggressive prostate cancer and antagonizes the SWI/SNF complex. *Nat Genet.* 2013;45(11):1392–8.
9. Mehra R, Udager AM, Ahearn TU, Cao X, Feng FY, Loda M, Petimar JS, Kantoff P, Mucci LA, Chinnaiyan AM. Overexpression of the long noncoding RNA SChLAP1 independently predicts lethal prostate cancer. *Eur Urol.* 2016;70(4):549.
10. Lee M, Kim HJ, Sang WK, Park SA, Chun KH, Cho NH, Yong SS, Kim YT. The long non-coding RNA HOTAIR increases tumour growth and invasion in cervical cancer by targeting the Notch pathway. *Oncotarget* 2016;7(28):44558–71.
11. Esteller M. Non-coding RNAs in human disease. *Nat Rev Genet.* 2011;12(12):861.
12. Tan S, Li R, Ding K, Lobie PE, Zhu T. miR-198 inhibits migration and invasion of hepatocellular carcinoma cells by targeting the HGF/c-MET pathway. *FEBS Lett.* 2011; 585(14):2229–34.
13. Yang J, Zhao H, Xin Y, Fan L. MicroRNA-198 inhibits proliferation and induces apoptosis of lung cancer cells via targeting FGFR1. *J Cell Biochem.* 2014;115(5):987.
14. Marin-Muller C, Li D, Bharadwaj U, Li M, Chen C, Hodges SE, Fisher WE, Mo Q, Hung MC, Yao Q. A tumorigenic factor interactome connected through tumor suppressor microRNA-198 in human pancreatic cancer. *Clin Cancer Res.* 2013;19(21):5901.
15. Shen J, Dicioccio R, Odunsi K, Lele SB, Zhao H. Novel genetic variants in miR-191 gene and familial ovarian cancer. *BMC Cancer* 2010;10(1):47.
16. Zhao JJ, Yang J, Lin J, Yao N, Zhu Y, Zheng J, Xu J, Cheng JQ, Lin JY, Ma X. Identification of miRNAs associated with tumorigenesis of retinoblastoma by miRNA microarray analysis. *Childs Nerv Syst.* 2009;25(1):13–20.
17. Qi B, Yao WJ, Zhao BS, Qin XG, Wang Y, Wang WJ, Wang TY, Liu SG, Li HC. Involvement of microRNA-198 overexpression in the poor prognosis of esophageal cancer. *Asian Pac J Cancer Prev.* 2013;14(9):5073–6.
18. Wang M, Wang J, Kong X, Chen H, Wang Y, Qin M, Lin Y, Chen H, Xu J, Hong J. MiR-198 represses tumor growth and metastasis in colorectal cancer by targeting fucosyl transferase 8. *Sci Rep.* 2014;4:6145.
19. Ye L, Li S, Ye D, Yang D, Yue F, Guo Y, Chen X, Chen F, Zhang J, Song X. Livin expression may be regulated by miR-198 in human prostate cancer cell lines. *Eur J Cancer* 2013;49(3):734–40.
20. Yang YT, Weng CJ, Ho CT, Yen GC. Resveratrol analog-3,5,4'-trimethoxy-trans-stilbene inhibits invasion of human lung adenocarcinoma cells by suppressing the MAPK pathway and decreasing matrix metalloproteinase-2 expression. *Mol Nutr Food Res.* 2009;53(3):407–16.
21. Huang Q, Wu LJ, Tashiro S, Onodera S, Li LH, Ikejima T. Silymarin augments human cervical cancer HeLa cell apoptosis via P38/JNK MAPK pathways in serum-free medium. *J Asian Natur Products Res.* 2005;7(5):701–9.
22. Davis JE, Xie X, Guo J, Huang W, Chu WM, Huang S, Teng Y, Wu G. ARF1 promotes prostate tumorigenesis via targeting oncogenic MAPK signaling. *Oncotarget* 2016;7(26):39834–45.
23. Paraskevopoulou MD, Georgakilas G, Kostoulas N, Reczko M, Maragkakis M, Dalamagas TM, Hatzigeorgiou AG. DIANA-LncBase: Experimentally verified and computationally predicted microRNA targets on long non-coding RNAs. *Nucleic Acids Res.* 2013;41(Database issue):239–45.
24. Zhang P, Singh A, Yegnasubramanian S, Esopi D, Kombairaju P, Bodas M, Wu H, Bova SG, Biswal S. Loss of kelch-like ECH-associated protein 1 function in prostate cancer cells causes chemoresistance and radioresistance and promotes tumor growth. *Mol Cancer Therapeut.* 2010;9(2):336–46.
25. Li W, Yu KN, Bao L, Shen J, Cheng C, Han W. Non-thermal plasma inhibits human cervical cancer HeLa cells invasiveness by suppressing the MAPK pathway and decreasing matrix metalloproteinase-9 expression. *Sci Rep.* 2016;6:19720.
26. Curran S, Murray GI. Matrix metalloproteinases: Molecular aspects of their roles in tumour invasion and metastasis. *Eur J Cancer* 2000;36(13 Spec No):1621–30.
27. Kim KJ, Li B, Winer J, Armanini M, Gillett N, Phillips HS, Ferrara N. Inhibition of vascular endothelial growth factor-induced angiogenesis suppresses tumour growth in vivo. *Nature* 1993;362(6423):841.

28. Mercer TR, Dinger ME, Mattick JS. Long non-coding RNAs: Insights into functions. *Nat Rev Genet.* 2009;10(3):155.
29. Zhang A, Zhang J, Kaipainen A, Lucas JM, Yang H. Long non-coding RNA, a newly deciphered “code” in prostate cancer. *Cancer Lett.* 2016;375(2):323–30.
30. Prensner JR, Iyer MK, Balbin OA, Dhanasekaran SM, Cao Q, Brenner JC, Laxman B, Asangani IA, Grasso CS, Kominsky HD. Transcriptome sequencing across a prostate cancer cohort identifies PCAT-1, an unannotated lincRNA implicated in disease progression. *Nat Biotechnol.* 2011;29(8):742.
31. Bussemakers MJ, Van BA, Verhaegh GW, Smit FP, Karthaus HF, Schalken JA, Debruyne FM, Ru N, Isaacs WB. DD3: A new prostate-specific gene, highly overexpressed in prostate cancer. *Cancer Res.* 1999;59(23):5975–9.
32. Zhang J, Shi Z, Nan Y, Li M. Inhibiting malignant phenotypes of the bladder cancer cells by silencing long noncoding RNA SChLAP1. *Int Urol Nephrol.* 2016;48(5):711–6.
33. Cui Z, Zheng X, Kong D. Decreased miR-198 expression and its prognostic significance in human gastric cancer. *World J Surg Oncol.* 2016;14(1):1–5.
34. Stelloo S, Sanders J, Nevedomskaya E, De JJ, Peters D, van Leenders GJ, Jenster G, Bergman AM, Zwart W. mTOR pathway activation is a favorable prognostic factor in human prostate adenocarcinoma. *Oncotarget* 2016;7(22): 32916–24.
35. Moro L, Arbini AA, Marra E, Greco M. [Corrigendum] Constitutive activation of MAPK/ERK inhibits prostate cancer cell proliferation through upregulation of BRCA2. *Int J Oncol.* 2007;30(1):217–24.
36. Li JX, Shen YQ, Cai BZ, Zhao J, Bai X, Lu YJ, Li XQ. Arsenic trioxide induces the apoptosis in vascular smooth muscle cells via increasing intracellular calcium and ROS formation. *Mol Biol Rep.* 2010;37(3):1569–76.
37. Roux PP, Blenis J. ERK and p38 MAPK-activated protein kinases: A family of protein kinases with diverse biological functions. *Microbiol Mol Biol Rev.* 2004;68(2):320–44.
38. Chun J, Kim YS. Platycodin D inhibits migration, invasion, and growth of MDA-MB-231 human breast cancer cells via suppression of EGFR-mediated Akt and MAPK pathways. *Chem Biol Interact.* 2013;205(3):212–21.